Study on Surrounding Rock Control and Support Stability of Ultra-Large Height Mining Face

Sheng Wang [1], **Xuelong Li** [1,*] and **Qizhi Qin** [1,2]

1   State Key Laboratory of Mining Disaster Prevention and Control, Shandong University of Science and Technology, Qingdao 266590, China
2   Yankuang Group Co., Ltd., Zoucheng 273500, China
*   Correspondence: lixl@sdust.edu.cn; Tel.: +86-195-0613-3256

Abstract: Surrounding rock control and support stability in the process of coal seam mining in ultra-large height mining face are the key to normal mine operation. In this study, the roof movement and deformation of an ultra-large height mining face are analyzed, and the working resistance of the ultra-large height mining face is obtained by introducing the equivalent immediate roof. By analyzing the coal wall spalling, the multiple positions of the spalling and the required support force of the support are obtained. At the same time, ultra-large height supports are more prone to instability problems. In this study, the stability of the ultra-large height supports was analyzed by establishing a mechanical model. The results show that: 1. The overturning limit angle of support has a hyperbolic relationship with the center of gravity. 2. Under the condition of ultra-large height, the increase in the base width of the bracket significantly improves the stability of the supports. 3. The sliding limit angle of support is positively correlated with the support load and the friction coefficient between the support and the floor. The above conclusions can provide guidance on the selection of supports and the adoption of measures to enhance the stability of the supports during use under ultra-large height conditions. The working resistance of the ultra-large height supports in the 108 mining face of the Jinjitan Coal Mine was monitored. The monitoring results show that: The average resistance of the supports is 22.6 MPa. The selected supports can meet the stability requirements of the working face support. The frequency of mining resistance in 0~5 MPa accounts for 28.38%, which indicates that some supports are insufficient for the initial support force during the moving process. Furthermore, the stability of the supports can be enhanced by adjusting the moving process. This study provides a reference for the selection of supports in ultra-large height mining faces and proposes measures to enhance the stability of the supports, which provides guidance for the safe mining of coal in ultra-large height mining faces.

Keywords: ultra-large height mining face; roof movement; support stability; control measures of surrounding rock; working resistance monitoring of supports

1. Introduction

Coal is the main global energy source [1,2]. With the development of science and technology, coal mining is developing towards the special direction of deep mining and high mining [3–5]. Large-height coal mining technology can significantly improve the coal recovery rate, which is an important development direction for the safe and efficient mining of thick coal seams [6]. The maximum mining height has now been developed to 8.8 m [7]. Scholars have undertaken a lot of related research on coal mining in large-height mining face. Li et al. [8] studied the problem of mine pressure in shallow mining faces with large mining heights and believed that the failure of key strata would trigger the fracture of sub-key strata, which would cause a greater load on the mining face. Lu et al. [9] found that the floor failure area of large-mining height mining faces is small and that the collapse of a large-mining height roof inhibits floor pressure relief. Ren et al. [10] studied the stress

distribution area of large-mining height working faces using theoretical calculation and numerical simulation. Liu et al. [11] studied the law of roof collapse and surface subsidence by establishing a three-dimensional geological model and a two-dimensional numerical simulation model.

In the process of coal mining, the support state of the mining face has a direct impact on the mining of coal resources [12,13]. Effective surrounding rock control is the premise of safe mining [14]. As one of the important ways to control the surrounding rock of the working face [15,16], supports have attracted the attention of many scholars. Due to the different occurrence conditions of coal seams, the relationship between the mining face support and the surrounding rock is complex and changeable [17,18]. Zeng [19] and Meng [20] established a numerical simulation model of hydraulic support by using ADAMS software and studied the motion trend and mechanical response of the hydraulic supports under impact load. Zhang et al. [21] and Xie [22] proposed that the combination of an advanced hydraulic support group and bolt (cable) constitutes an advanced coupling support system. Cheng et al. [23] and Wang et al. [24] used numerical simulation to analyze the loading and operating characteristics of hydraulic supports, the influence of depression angle on mining pressure characteristics, and the relationship between the propulsion speed and the support loading.

At the same time, large-height mining faces are also faced with problems such as roof collapse and strong ground pressure disasters [25,26]. With the development of the mining height to 6~7 m, the probability of instability disasters in the stope support–surrounding rock is significantly increased [27,28]. For large-height mining faces, the stability problem of support–surrounding rock is more prominent [29]. Yuan [30] proposed a surrounding rock control scheme combining a high pre-stressed anchorage structure and an automatic advance hydraulic support for the problem of large deformation in roadways during excavation and the mining of large-height mining faces. Zhang et al. [31] studied the effect of hydraulic supports and surrounding rock in large-height mining faces based on the continuous–discontinuous element method (CDEM). Meng [32] established the mathematical model of the bearing capacity area of the support under different load conditions and studied the support failure mechanism of the large mining height power support based on the dynamic numerical simulation model of ADAMS software. Wu et al. [33], through simulation, theoretical analysis, and field measurement, analyzed the roof crushing structure form of large-height mining faces and the calculation method of reasonable support resistance of the supports. Pang [34] established a tensile-cracking–sliding dynamic model of coal wall spalling for large-height mining faces and calculated the critical protection force. Li Heng et al. [35] studied the influence law of the stability of the coal wall of the large-height mining hydraulic supports by combining theoretical analysis and numerical simulation.

Many scholars have studied the working resistance and stability of large-height mining supports by theoretical derivation, numerical simulation, and model tests. However, there are still few studies on the relationship between the supports and the surrounding rock in ultra-large height mining faces with a mining height of more than 7 m. Based on the existing research, this paper summarizes and discusses the support–surrounding rock control technology of ultra-large height mining faces [36–38]. The roof movement of an ultra-large height mining face is analyzed, and the stability model of the ultra-large height support is established. The support selection for an ultra-large height mining face is guided by studying the influence of field factors on the support stability. This study provides a reference for the selection of supports in ultra-large height mining faces and proposes measures to enhance the stability of the supports, providing guidance for the safe mining of coal in ultra-large height mining faces.

2. Support—Surrounding Rock Control Technology of Ultra-Large Height Mining Face

2.1. Roof Movement Deformation Mechanism of Ultra-Large Height Mining Face

The roof movement process is actually a dynamic load process in which the roof rock layer takes the coal wall as the fulcrum and rotates and sinks under its own gravity (Figure 1). The roof fracture form is a layer-by-layer fracture [5]. Therefore, when the roof has catastrophe instability, according to the moment equilibrium condition, the force of the roof on the stope support (*R*) [39] is:

$$R = \frac{m\gamma L^2}{L_k} \tag{1}$$

where, the height of the roof falling zone [40] is $m = \frac{100\sum h}{4.7\sum h + 19} \pm 2.2$; γ is the weight density of rock, t/m^3; C is the periodic fracture of the rock stratum instability distance, m; L_0 is the primary fracture of the rock stratum instability distance, m; L_k is the roof distance, m.
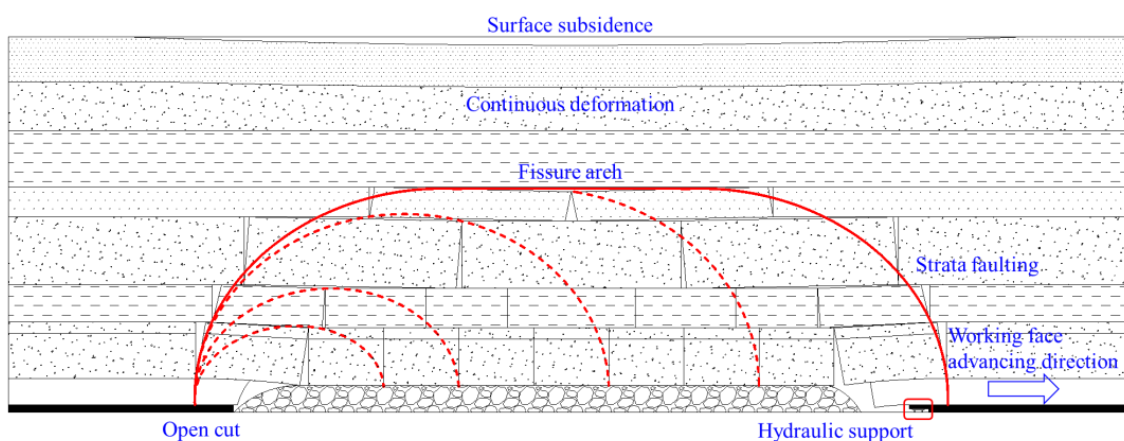

Figure 1. Mechanical model diagram of roof effect on stope supports.

Under the conditions of ultra-large mining height, the increase in the mining height has a great influence on the fracture and collapse of the overlying rock on the mining face, and the immediate roof fracture and falling backward have poor filling effects on the mined-out area. The movement space of the upper main roof increases with the increase in the mining height. This necessitates further requirements for the mining resistance of the mining face supports [41,42].

Due to ultra-large height mining faces, mining thickness increased, the original immediate roof cannot fill the goaf, and the lower group of the main roof layer collapses backward and cannot form a hinge structure; it is a caving state, equivalent to the role of the immediate roof. Therefore, the immediate roof of the mining face with an ultra-large mining height should be redefined. The rock stratum between the coal seam and the hinged main roof, which cannot form a structure, is called the equivalent immediate roof.

The immediate roof has an important influence on the support load. Due to the thick equivalent immediate roof, if the immediate roof strength is low or the support resistance is insufficient, under the action of the self-weight of the thick immediate roof, the mining face will continue to be in a high resistance state. In order to prevent immediate roof damage, the timely provision of adequate support is required. Therefore, ultra-large mining height support is required to have a high setting load and working resistance to balance the weight of the immediate roof and the load of the main roof structure.

2.2. Support–Surrounding Rock Relationship

The interaction between the support and the surrounding rock includes the control mode of the support to the immediate roof and the control mode of the main roof rock beam. The two are the two sides of the contradiction, in which the surrounding rock is

the main body, and the support is the passive body. Under the condition of ultra-large mining height, because the immediate roof may have a large-span suspended roof structure, accurately grasping the on-site working conditions is the key to the roof control design and support selection calculation of ultra-large mining height.

After the excavation of the coal seam in the working face, the equilibrium state of the original rock stress field in the rock mass is destroyed. Under the action of the mining stress field, the roof strata undergo periodic irregular failure and instability. The hydraulic support is used as the supporting structure of the working face to support the roof, protect the coal wall, and isolate the caving gangue in the goaf. The supporting stress field and the mining stress field are coupled to form a dynamic equilibrium. Based on the coupling characteristics of the mining stress field of the surrounding rock and the supporting stress field of the hydraulic support, the coupling relationship between the hydraulic support and the surrounding rock can be divided into strength coupling, stiffness coupling, and stability coupling, as shown in Figure 2.
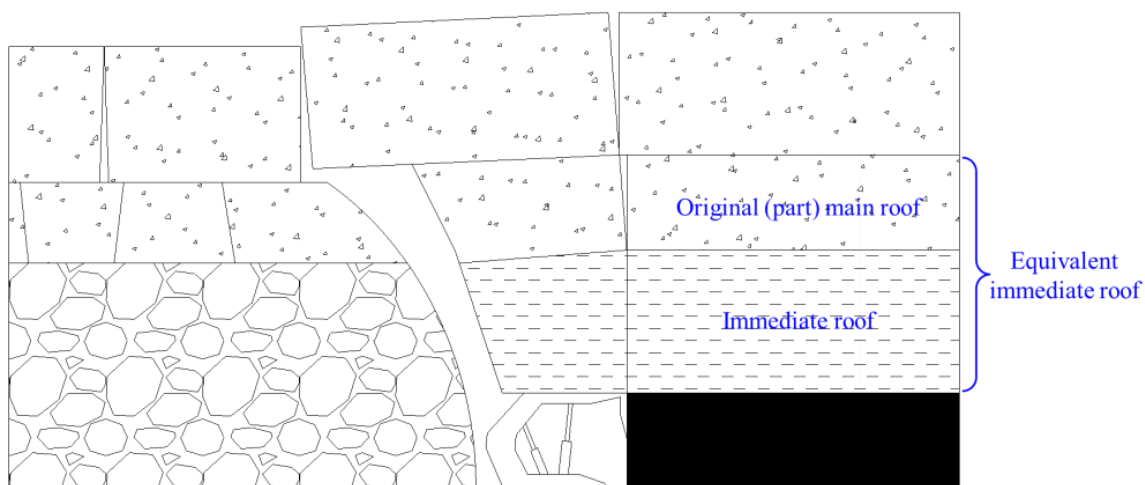

Figure 2. Schematic diagram of equivalent immediate roof of ultra-large height mining face.

The equilibrium state of the in situ stress field in the rock mass is destroyed after the excavation of the coal seam. Under the action of the mining stress field, the roof strata are periodically and irregularly damaged and destabilized. The hydraulic support is used as the supporting structure of the working face to support the roof, protect the coal wall, and isolate the falling gangue in the goaf. The supporting stress field and the mining stress field are coupled to form a dynamic balance. Based on the coupling characteristics of the mining stress field of the surrounding rock and the supporting stress field of the hydraulic support, the coupling relationship between the hydraulic support and the surrounding rock can be subdivided into strength coupling, stiffness coupling, and stability coupling [37].

Reasonable determination of support working resistance is the top priority in dealing with the relationship between the support and the surrounding rock. The traditional calculation of support working resistance is mainly divided into given deformation and limited deformation. Under the condition of a given deformation scheme, the support can only reduce the movement speed of the rock beam within a certain range, but it cannot prevent the movement of the rock beam. At this point, the support resistance does not need to exceed the sum of the immediate roof force (A) and the rock beam sinking to the bottom to the support force (K_A).

$$P_{T\max} = A + K_A \tag{2}$$

where, $K_A = \frac{m_E L' \gamma_E}{2 K_T l_K}$; m_E is the thickness of the main roof rock beam, m; γ_z is the density of main top rock beam bulk, kg/m^3; L' is the initial instability distance of the main roof rock beam, m; K_T is the proportional coefficient considering the weight of the rock beam.

Under the condition of limited deformation, it is required to control the roof subsidence of the stope (Δh_T), and it must be less than the roof subsidence of the stope (Δh_A) when the rock beam is broken. Assuming that the stope is in a relatively balanced and stable state, the potential state equation is established according to the mechanical balance, and the maximum support strength $P_{T\max}$ is:

$$P_{T\max} = A + K_A \frac{\Delta h_A}{\Delta h_T} \tag{3}$$

The influence of the mining height must be considered in the calculation of the working resistance of large-mining height supports. With the increase in mining height, the range of the subsidence area of the roof is also expanded, which leads to the working resistance of the supports being much higher than that of general mining height supports. Some scholars, specifically for large-mining heights under the condition of fully mechanized working resistance, put forward this relevant calculation equation [41]:

$$R = \left[P_0 f\left(\frac{L}{2} + 0.5H\cot\alpha\right) + P_H f\left(\frac{l}{2} + 0.5h\cot\alpha\right) - (Ks_2 - Q_B)(H - s_1 - c - H\sin\alpha)\right] / (fc) \tag{4}$$

where R is the working resistance of the large-mining height support, N; P_0 is the gravity of the main roof rock, N; f is the friction factor between the rocks; H, L is the thickness and collapse step of the main roof, m; α is the angle of fracture, °; P_H is the gravity of the immediate roof rock, N; h, l is the thickness and collapse step of the immediate roof, m; K is the stiffness of the waste rock in the mined-out area N/m; s_2 is the compression quantity of the waste rock in the mined-out area, m; Q_B is the gravity of the immediate roof rock just in contact with the waste rock, N; s_1 is the subsidence of the main roof rock, m; c is the position of the support force.

At the same time, in the calculation of support selection, due to the large mining height and the hard roof, there is insufficient gangue as a cushion in the mined-out area after the roof fracture. Therefore, in the process of the rapid sinking of the movable column, it is easy to cause a large amount of liquid to damage the hydraulic valve of the hydraulic support. Therefore, it is necessary to improve the hydraulic control valve of the traditional support in the selection of the support to ensure that the hydraulic control valve is released in time to avoid the hydraulic control valve from being damaged by a large impact force.

2.3. Analysis of Coal Wall Spalling Mechanism of Ultra-Large Height Mining Face

With the increase in mining height, the probability of coal wall spalling also increases. Serious coal wall spalling has a great influence on the normal production of super-large mining height working face. First of all, the coal wall spalling seriously affects the safety of personnel and the normal production work; secondly, after coal wall spalling, the empty roof distance increases, which easily leads to the deterioration of the roof conditions; finally, coal wall spalling will also lead to uneven stress on the support and poor roof connection. Preventing coal wall spalling is an important means to ensure the normal production of ultra-large height mining faces.

The coal wall under the horizontal extrusion pressure and the roof pressure from the coal in front of the working face can be considered as a fixed end, a simply supported end, or a free end equal to the section beam. The relationship between the frictional resistance F_f between the coal seam (mining height h) and the roof and floor and the uniform load qh is established: $Z = qh - F_f$, and the simplified mechanical model is shown in Figure 3.
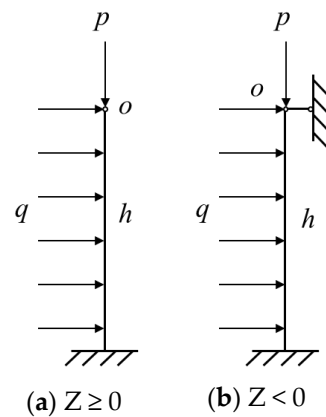
Figure 3. Simplified mechanical model of coal wall spalling.

When $Z \geq 0$, the coal wall spalling model can be seen as a cantilever beam with one end fixed and one end free. Point o is taken as the origin of the coordinate, the vertical downward is the x-axis, and the horizontal right is the y-axis, and a plane rectangular coordinate system is established for force analysis.

Take the moment of the centroid of any x-section:

$$M + \frac{1}{2}qx^2 = 0 \tag{5}$$

According to material mechanics, the approximate differential equation of the deflection curve is:

$$\omega'' = \frac{qx^2}{2EI} \tag{6}$$

The deflection equation can be obtained by integrating the Equation (6):

$$\omega = \frac{qx^4}{24EI} - \frac{qxh^3}{6EI} + \frac{qh^4}{8EI} \tag{7}$$

The maximum deflection value point of the coal wall occurs at the contact between the coal seam and the roof, that is, the mining height. The deflection value at this point is:

$$\omega_{\max} = \frac{qh^4}{8EI} \tag{8}$$

When $Z < 0$, the coal wall spalling model can be seen as a fixed-end, one end simply supports the beam. Because it is a statically indeterminate beam, the superposition principle can be used to calculate deflection. The deflection of the cantilever beam under uniform load and roof pressure and the deflection of the cantilever beam under concentrated load and roof pressure at point o is zero:

$$\frac{qh^4}{8EI} - \frac{F_y l^3}{3EI} = 0 \tag{9}$$

$$F_y = \frac{3}{8}ql \tag{10}$$

For any x-section centroid, it can be found that:

$$M = \frac{3qhx}{8} - \frac{qx^2}{2} \tag{11}$$

When $x = \frac{1+\sqrt{33}}{16}h$, that is, 0.578 times of the mining height, the maximum deflection value is:

$$\omega_{\max} = \frac{13qh^4}{2400EI} \tag{12}$$

Based on the above research, it can be concluded that coal wall spalling generally occurs in the upper part of the mining height. So is the actual observation through the field. Based on the mechanical conditions of the surrounding rock of the 8.0 m ultra-large height mining face in the coal seam, the deflection characteristics of the coal wall are analyzed by the pressure bar theory. It is found that the position of the coal wall prone to spalling is in the middle and upper part of the coal wall, which is about 5.2 m away from the floor. The protective force should not be less than 0.245 MPa. According to the observation of actual production on-site, the rib spalling position of the coal wall is in the middle and upper part, and the damage depth of the coal wall is about 1.0~1.3 m.

3. Stability Analysis of Supports

3.1. Overturning Stability Analysis of Ultra-Large Height Mining Face

Good support–surrounding rock relationship is an important way of guaranteeing the high yield and high efficiency of the mining face. The ultra-large mining height support itself is high and heavy, and its structural stability is worse than that of the ordinary mining height support. Serious support stability problems are prone to occur during the operation of the support. The stability problems of ultra-large mining height support can be divided into two categories: the support overturning problem and the support sliding problem. The stability problem of ultra-large mining height supports can be simplified, as shown in Figure 4.
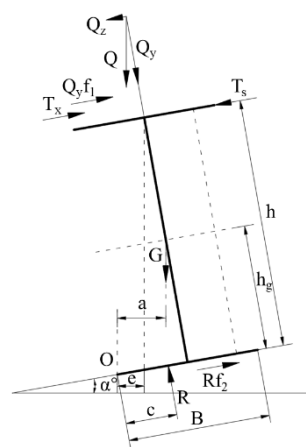

Figure 4. Static scheme of the support unit.

In Figure 4, Q is the support subjected to the combined force of the roof pressure; G is the weight of the support; T_S and T_X are the upper and lower adjacent supports' extrusion force; R is the resultant floor force; $Q_y f_1$ and Rf_2 are the friction between the support and the roof—floor; f_1, f_2 are the friction coefficients of the roof and floor. h is the height of the support, m; a is the vertical distance from point O to the gravity line of the support center, m; c is the distance from point O to gravity action line of support center of gravity on support base, m; e is the vertical distance from point O to the roof force, m; The supports are in equilibrium under the action of the above force. Take the moment of point O on the lower side of the support base:

$$T_s h + Rc = Qe + Ga + hQ_y f_1 + T_x h \tag{13}$$

When the support is not connected to the top, $T_S = T_X = 0$, $Q = 0$. According to Equation (13) $Rc = Ga$. The support is in limit equilibrium when the center of gravity line of the support passes through point O. Where upon, $a = 0$, $\frac{B}{2}\cos\alpha - h_g \cdot \sin\alpha = 0$. It can

be seen that support overturning is related to the inclination angle, support base width, and support center height. The larger the inclination angle, the higher the support gravity center height, and the easier the support overturning. The width of the ultra-large mining height supports base is generally 2.05 m. The relationship between the height of the center of gravity and the inclination angle is shown in Figure 5. Above the curve is the overturned area, and below the curve is the stability area.
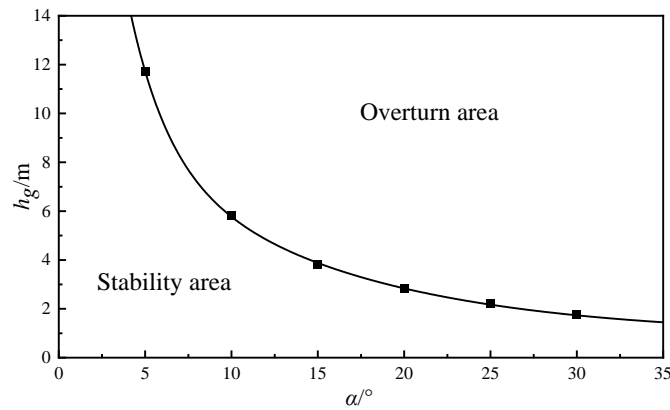

Figure 5. Relationship between height of support unit gravity center h_g and limit angle α.

From Figure 5, it can be seen that the relationship between the overturning limit angle and the height of the center of gravity is hyperbolic in the support state. Under the same mining height, the higher the center of gravity, the smaller the limit angle. When the height of the center of gravity is less than 3.83 m, the trace of the center of gravity is reduced, which can cause the limit angle to significantly increase. Therefore, reducing the height of the center of gravity can effectively prevent the supports from overturning.

Making assumptions: ① the canopy is subjected to uniform load along the inclined direction; ② the floor pressure on the base is distributed uniformly along the inclined direction; ③ $T_x = T_s$ (see Figure 4). When the support is in contact with the roof, according to the torque balance analysis, according to Equation (13), there is $Rc + Qe = Ga + hQ_yf_1$. c is a certain value between 0–$B/2$; Q_y is the component force of Q value perpendicular to the canopy plane, $Q_y = Q\cos\alpha$; f_1 is the friction coefficient between the roof and the canopy, which has a large variation range with different contact conditions when using 0.3. When the support may be in a critical state, the roof pressure action line should be located on the left side of point O ($h\sin\alpha - \frac{B}{2}\cos\alpha > 0$), and the self-weight action line should be located on the right side of point O ($\frac{B}{2}\cos\alpha - h_g\sin\alpha > 0$), then

$$Q(h\sin\alpha - 0.5B\cos\alpha - 0.3h\cos\alpha) = G(0.5\cos\alpha - h_g\sin\alpha) \tag{14}$$

$$\mathrm{arctg}\left(\frac{B}{2h}\right) < \alpha < \mathrm{arctg}\left(\frac{B}{2h_g}\right) \tag{15}$$

When α is less than the lower limit value, the roof force Q and the self-weight G action line do not exceed the O point. When α is greater than the upper limit value, the above two forces exceed the O point. In Equation (15), let $h_g = 0.4h$. When the calculated h value takes different values, the variation range of the α value is shown in Table 1. With the increase in the mining height, the upper and lower limits of α decrease, and the limit angle is very sensitive to the change in the mining height.

Table 1. Changes of α value at different h values.

h/m	3.6	4.6	5.6	6.6	7.6
$\alpha/^\circ$	15.9–35.4	12.6–29.1	10.4–24.6	8.8–21.2	7.7–18.6

If $Q > Q_{cr} = G \cdot \frac{(0.5\cos\alpha - h_g \sin\alpha)}{(h\sin\alpha - 0.5B\cos\alpha - 0.3h\cos\alpha)}$, the supports unit will overturn otherwise it will not overturn. The critical value of the roof load $-Q_{cr}$ results from Equation (14). Let $\lambda = Q/G$, $Q_g = 18{,}000$ kN, $G = 700$ kN, then the variation range of λ is 0–25.7. Assuming that the width of the support is 2.05 m, the h-α relationship determined by Equation (14) is shown in Figure 6.
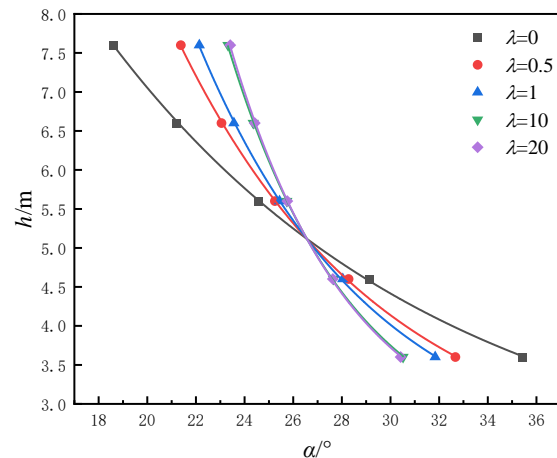

Figure 6. Relationship between support height h and limit angle α.

It can be seen from Figure 6 that when the support is in a supporting state, the collapse of the support is not only related to the height of the center of gravity but also related to the actual support height h of the support. The relationship between h and the limit angle α is curvilinear. The larger the support height, the smaller the limit angle. The higher the support height, the greater the limit angle decreases. The relationship between the mining height of the support and the limit angle is affected by the external load of the roof (λ). When the support is lifted to the initial support state, the support is subjected to the force of the roof on the support perpendicular to the canopy, which helps to prevent the support from overturning. When the support is in a passive support state, the support is affected by the gravity of the roof along the direction parallel to the canopy, and the limit angle α value varies with the mining height. When the mining height is less than 4.9 m, the α value decreases with the increase in the roof pressure (λ increases). When the mining height is greater than 4.9 m, as the top pressure increases (λ increases), the limit angle increases, and the higher the mining height, the greater the increase in α with the external load. Combined with Table 1, it can be seen that with the increase in mining height, the upper and lower limit angles become smaller, and the range becomes smaller. This shows from another point of view that the ultra-large mining height support is very sensitive to the angle, and it is easy to change from a stable state to an unstable state. It has poor adaptability to the change of coal seam angle and can prevent overturning by connecting the roof and moving the support.

Obviously, the support width will affect the overturning characteristics of the support, and the α-B relationship at a mining height of 4.6 m is shown in Figure 7. The wider the support is, the larger the limit angle is, regardless of the mining height, and the influence of width decreases with the increase in the support load. Similarly, the variation of h with the increase in B is investigated at the limit angle of $h = 4.6$ m and 6.6 m. As shown in Figure 8, it can be seen that as the width of the support increases, the limit height of the support also increases linearly. Increasing the support width can effectively increase the upper limit of the support height. In other words, the range of the wide support to adapt to the inclination of the coal seam is large. At the same time, with the increase in the mining height, the contribution rate of support width increases. Therefore, in the case of ultra-large mining height, increasing the support width has practical significance. Under the existing support width, it can be effectively prevented by adding a connecting jack between the supports, which is equivalent to increasing the width of the base.
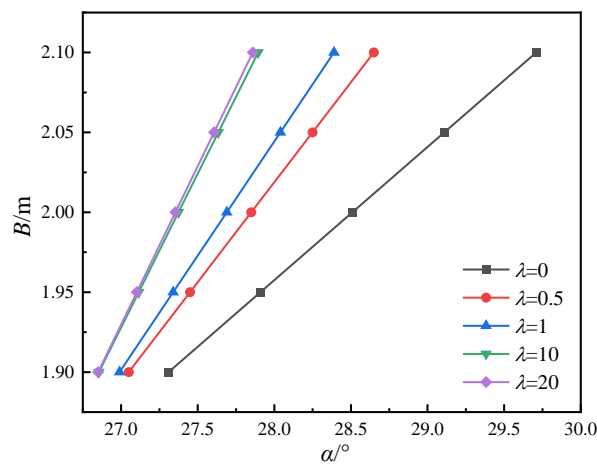
Figure 7. Relationship between support width *B* and limit angle α.
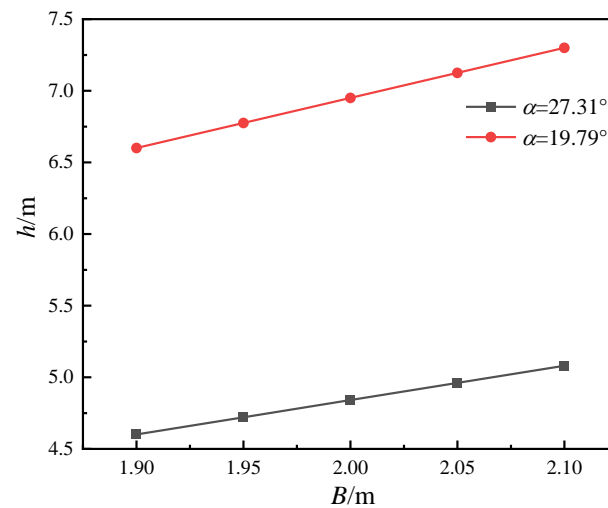

Figure 8. Relationship between mining height *h* and width *B*.

The difference between the free state and the single support is that the mining face supports are generally closely arranged, and the canopy will be subjected to the force T_S and T_X of the upper and lower adjacent supports. Under the normal support state of the mining face, when the support does not exceed the overturning limit angle, each support is in a stable state and will not be overturned. $T_S = T_X$; that is, the canopy of the support is not affected by the force of the canopy of the adjacent support. On the contrary, when the supports are overturned, the support must bear the force T_S of the upper adjacent support due to the overturning trend and also give the lower adjacent support force T_X. Assume that the first bracket on the upper end has a tendency to overturn $T_S = 0$; in order to prevent it from overturning, the second bracket must provide T_S, the expression is:

$$T_{x(1-2)} = Q \sin \alpha + \frac{h_g}{h} G \sin \alpha - Q f_1 \cos \alpha - (Q + G) \frac{B}{2h} \cos \alpha \tag{16}$$

where, $h = 6.6$ m, $h_g/h = 0.4$, $f_1 = 0.3$, $B = 2.05$ m, $G = 700$ kN, $\lambda = Q/G$, and α exceeds the limit angle corresponding to λ, the T_S value is shown in Figure 9.
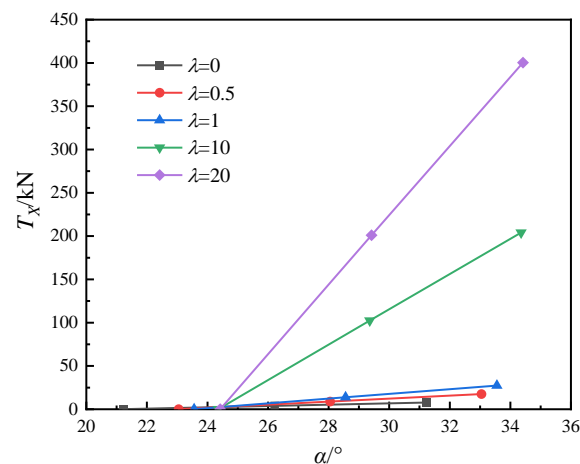
Figure 9. Relationship between force T_X between supports and limit angle α.

In this case, T_X is related to the value of α and λ. The larger the value of λ is (the greater the roof pressure is), the greater the lateral force of the lower support under the upper support is. When λ exceeds 1, the value of T_X increases sharply. In order to realize the balance of the support in the whole working face, the last support of the lower end must provide the lateral thrust of n $T_{x(1-2)}$. Therefore, comprehensive measures should be taken to prevent overturning. The thrust is applied at the end as follows, and the tension is applied at the upper end. The field can be realized through the section of the mining face.

From the perspective of anti-overturning ability, the support structure should have a low center of gravity and a wide base. From the perspective of adapting to geological conditions, the roof should be moderately stable, and the fluctuation of the roof and floor is small. From the operation, the supports should be lowered, fast-moving supports, and fast-lifting supports.

3.2. Stability Analysis of Support Sliding in Super High Mining Face

The lateral decline of the support refers to the decline of the support along the mining face. When the current sliding force is greater than the maximum friction force of the support, the support has a downward trend. In the critical state, it is as follows:

$$Q \cos \alpha \cdot f_1 + T_x + (Q + G) \cdot \cos \alpha \cdot f_2 = (Q + G) \sin \alpha + T_s \tag{17}$$

The sliding characteristics of single support are divided into two cases: ① The support is not connected ($Q = 0$), and $T_s = T_x = 0$; ② the support joint ($Q \neq 0$), and $T_s = T_x = 0$.

When the support is not attached, according to Equation (17), there are $G \cos \alpha f_2 = G \sin \alpha$, critical angle $\alpha = \text{arctg} f_2$. Obviously, whether the support falls at this time is only related to the friction coefficient between the support and the floor. When $f_2 = 0.4$, the critical angle $\alpha = 21.8°$. Compared with the critical angle of overturning (α_o) when the support is not connected to the roof, when the mining height is 4.6 m or 5.6 m, the critical angle of overturning is 27.63° or 24.59°, which are greater than the critical angle of sliding. Therefore, the support first falls and loses stability. The critical angle of sliding (α_s) should be taken as the critical angle of stability of the support. When the mining heights are 6.6 m and 7.6 m, the critical angles of overturning are 21.22° and 18.63°, which are less than the critical angle of sliding. The support first overturns, and the critical angle of overturning should be taken as the critical angle of stability of the support (α). The effect of the friction coefficient on the critical angle stability of the lateral stability of a single support without top contact is shown in Table 2.

Table 2. Relationship between support–floor friction f_2 and critical angle α of lateral stability of single support.

| h		4.6 m	5.6 m	6.6 m	7.6 m
α_o		27.63°	24.59°	21.22°	18.63°
$f_2 = 0.2$	α_s	11.3°	11.3°	11.3°	11.3°
	α	11.3°	11.3°	11.3°	11.3°
$f_2 = 0.3$	α_s	16.7°	16.7°	16.7°	16.7°
	α	16.7°	16.7°	16.7°	16.7°
$f_2 = 0.4$	α_s	21.8°	21.8°	21.8°	21.8°
	α	21.8°	21.8°	21.22°	18.63°
$f_2 = 0.5$	α_s	26.6°	26.6°	26.6°	26.6°
	α	26.6°	24.59°	21.22°	18.63°
$f_2 = 0.6$	α_s	31°	31°	31°	31°
	α	27.63°	24.59°	21.22°	18.63°

When the single support is connected to the top, in this case, $T_S = T_X = 0$, but $Q \neq 0$, according to Equation (17), there is

$$Q \cos \alpha f_1 + (Q + G) \cdot \cos \alpha f_2 = (Q + G) \sin \alpha \qquad (18)$$

The value of f_1 also changes with the roof lithology and roof conditions, but this value is relatively stable compared with f_2, and the set value is 0.3. At the same time, let $\lambda = \frac{Q}{G}$, there is:

$$\alpha = arctg\left(f_2 + \frac{\lambda}{1+\lambda} f_1\right) \qquad (19)$$

By Equation (19), the critical slip angle at the top of the single support is not only related to the friction coefficient between the support and the floor but also to the support load. At different times, the relationship between the friction f_2 and the limit angle α is shown in Figure 10. The relationship between the friction f_2 and the limit angle α at different λ is shown in Figure 10.
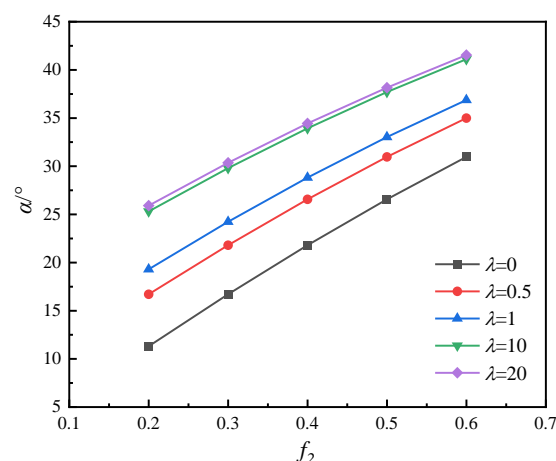
Figure 10. Relationship between limit angle α and support–floor friction f_2.

It can be seen from Figure 10 that no matter how the support is loaded, the limit angle α increases with the increase in the f_2 value, and the increasing f_2 value can effectively prevent sliding. With the increase in roof pressure, the limit angle increases, but it does not increase linearly. The greater the roof pressure, the smaller the increase. The smaller the value of the friction coefficient f_2, the greater the increase in the limit angle with the increase in λ is than that with the larger value of f_2. Therefore, moving support with pressure is an important measure for anti-sliding. The greater the pressure is, the better the anti-sliding effect is. For the mining face with a broken roof, it is very likely to cause roof caving. The

limit angle of $\lambda = 0$ should be used as the limit angle under this condition. For the roof above medium stability, the limit angle of $\lambda = 0.5$ or $\lambda = 1$ can be used as the limit angle under this condition when the management is good. The smaller the friction coefficient f_2, the greater the increase is.

The difference between multiple sliding and single sliding is that the sliding of the support is affected by the extrusion force T_X and T_S of the upper and lower adjacent supports. Before reaching the sliding limit angle of the single support, there is no sliding on the single support, and the force connection between the upper and lower supports is $T_X = T_S = 0$. After exceeding the sliding limit angle of the support, the support slides and the upper support produces the extrusion force on the lower bracket. In order to distinguish the extrusion force from the overturning, the extrusion force generated by the slide is expressed by T_X slide and T_S slide. Assuming that the first shelf at the upper end falls, the force on the second is:

$$T_{x(1-2)\text{slide}} = (Q + G)\sin\alpha - [(Q + G)f_2 + Qf_1]\cos\alpha \tag{20}$$

The sliding force of the whole mining face supports is:

$$\text{n}T_{x(1-2)\text{slide}} = \text{n}(Q + G)\sin\alpha - \text{n}[(Q + G)f_2 + Qf_1]\cos\alpha \tag{21}$$

where, n is the number of supports in working face.

The force that should be provided at the lower end of the support to prevent the sliding of the mining face is $F_{kh} = \text{n}T_{x(1-2)slide}$, let n = 147, $f_2 = 0.3$, $G = 700$ kN. When calculating the limit angle when α exceeds $\lambda = 0$, the relationship between α and F_{kh} is shown in Table 3.

Table 3. The relationship between F_{kh} and limit angle α under.

α	16.7°	24.2°	29.8°	30.4°
F_{kh}	0	14,079.70 kN	24,350.70 kN	25,372.20 kN

It can be seen from Table 3 that with the increase in the angle beyond the critical angle, the anti-sliding force that must be provided increases. With an average increase of 1°, the anti-sliding force increases by 1852 kN. In the process of support installation, the supports should be connected to the top, and the initial support force should be generally achieved. Therefore, the possibility of an overall decline in the mining face is slight and easy to control, which is not the main contradiction of anti-sliding. The decline of the mining face supports is the decline of the other supports caused by the decline of the individual supports.

3.3. Factors Influencing the Stability of Super High Mining Face

There are many factors affecting the support stability of ultra-large height mining faces, which can be summarized into two categories, geological conditions and support structure design. In the geological conditions, the dip angle of the coal seam, the complex geological structure, and the strength of the coal seam (the degree of coal wall spalling) affect the stability of the supports to different degrees. From the perspective of the support structure, the support type, the initial support force and the mining resistance, the position of the center of gravity of the supports, and the configuration of the anti-slide and anti-skid device of the support all affect the stability of the supports. The above factors have a more obvious influence on the ultra-large height mining face. The stability of the support should mainly consider the following factors.

(1) Mining face inclination angle

In the mining face with a large dip angle, sliding and dumping may occur when the supports are moved. The sliding is due to the gravity of the supports being greater than the friction between the support base and the floor, and the dumping is due to the gravity center of the support exceeding the support base. In actual production, due to the

dense arrangement between the canopies of the supports, there are constraints between the canopies and the side shield, and the gap between the base is large, which leads to the sliding of the base and the upward dumping of the support.

(2)　Support structure

The support with ultra-large mining height has a large weight and a high center of gravity, and the stability of the support becomes worse when the width of the support changes little.

(3)　Stress state of support

It is closely related to the state of the roof and floor and also related to the support type and mining resistance. When the roof sinks, if there is a movement in the inclined direction, the supports are subjected to the force along the inclined direction, which will drive the support to tilt downward. If the control of the support is unreasonable, roof leakage occurs, the stress of the support deteriorates, and the supports are subjected to eccentric load or loss of restraint, which also makes the supports unstable. In addition, when the roof and floor are uneven, the canopy and the base are poor, and the support's capacity cannot be fully exerted. When the roof deformation is large, it may lead to steps between the canopies, causing biting and dumping. When there is water in the roof and floor of the working face, the friction between the roof and floor decreases, which intensifies the influence on support dumping.

4. Application of Super-Large Mining Height Fully Mechanized Support

4.1. Overview of Working Face

The 108 mining face of the Jinjitan Coal Mine (Figure 11) is the first mining face in the southwest of the first panel. The coal seam thickness is 5.5~8.4 m, and the average dip angle is less than 1°. The overall trend is a monoclinic structure tilted to the northwest, without fold and magmatic activity. The mining face with ultra-large height mining technology, a designed mining height of 5.8~8.2 m, is deeper than less than 50 times. The mining face with a buried depth of 239~252 m, an overall east high west low, south high north low, and an average angle of 5~8°. The 108 mining face length is 300 m, and the maximum mining height is 7.8 m. The 108 mining face operators plan to use large mining height for full-seam mining equipment; the mining length of the design is 5227.4 m.
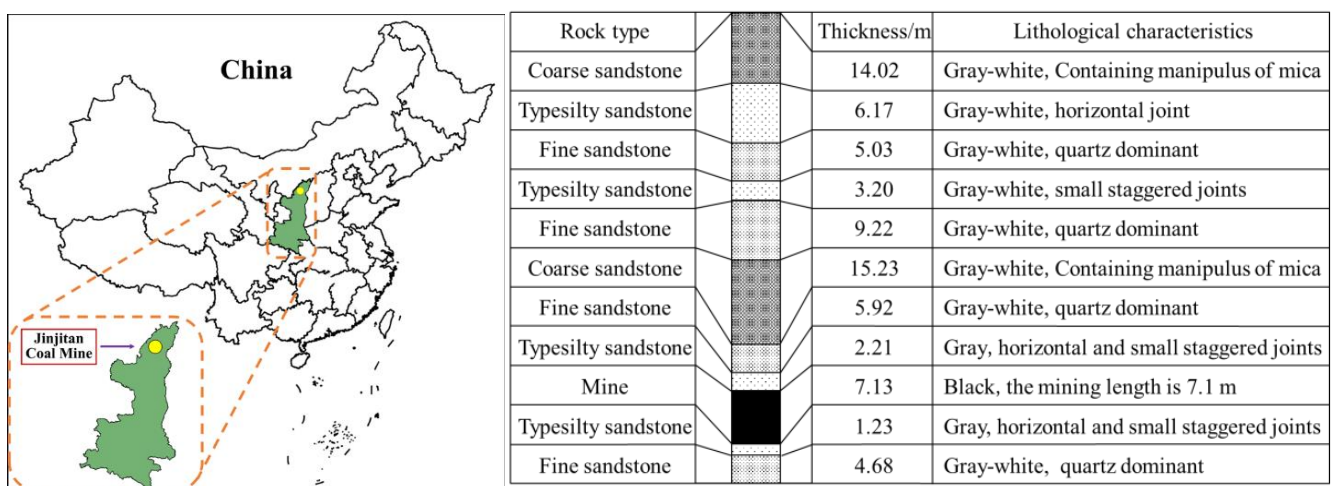

Rock type			Thickness/m	Lithological characteristics
Coarse sandstone			14.02	Gray-white, Containing manipulus of mica
Typesilty sandstone			6.17	Gray-white, horizontal joint
Fine sandstone			5.03	Gray-white, quartz dominant
Typesilty sandstone			3.20	Gray-white, small staggered joints
Fine sandstone			9.22	Gray-white, quartz dominant
Coarse sandstone			15.23	Gray-white, Containing manipulus of mica
Fine sandstone			5.92	Gray-white, quartz dominant
Typesilty sandstone			2.21	Gray, horizontal and small staggered joints
Mine			7.13	Black, the mining length is 7.1 m
Typesilty sandstone			1.23	Gray, horizontal and small staggered joints
Fine sandstone			4.68	Gray-white, quartz dominant

Figure 11. Location map of Jinjitan coal mine and strata map of mining face.

4.2. Determination of Support Parameters

(1)　First fracture of main rock beam

The on-site measured data, m_E = 15.87 m, C_1 = 66 m, L_k = 5.9 m, γ_E = 2.5 t/m^3, S_T = 11.8 m^2, meet the control requirements of the first fracture time of the lower rock beam of the main roof support strength P_T

$$P_T = m_E \cdot \gamma_E + \frac{m_E \cdot \gamma_E \cdot C_1}{2l_k} \tag{22}$$

Support working resistance $R_T = P_T \times S_T$, the lower limit: R_{Tmin} = 4681 kN; upper limit: R_{Tmax} = 26,184 kN.

(2)　Periodic fracture of main rock beam

Taking C_Z = 30 m, Δh_T = 1.53 m, the support strength and impedance force must meet the following requirements:

$$P_T = m_E \cdot \gamma_E + \frac{m_E \times r_E \times C_Z}{2l_k} \cdot \frac{\Delta h_A}{\Delta h_T} \tag{23}$$

where Δh_T is the required control of stope roof subsidence value. According to the actual situation of the existence of 'internal stress field', the lower limit: $h_T = \Delta h_A$, then P_{Tmin} = 140.535 t/m^2; upper limit: Δh_T = 0.75 Δh_A, then P_{Tmax} = 173.8 t/m^2. Lower limit of working resistance of support: R_{Tmin} = 16,583 kN; upper limit: R_{Tmax} = 20,508.4 kN.

(3)　Determination of support strength

According to the theoretical analysis and field formation data, there are two rock beams that have an obvious influence on the strata behavior of the stope. The first rock beam is fine-grained sandstone with an average thickness of 19.55 m. The initial mutation instability (initial movement) step is about 91 m, and the periodic mutation instability (periodic movement) step is about 27 m. The second rock beam is a medium-grained sandstone with an average thickness of 22.45 m. Its initial mutation instability (initial motion) step is 122 m, and the periodic mutation instability (periodic motion) step is 30 m.

The requirement of the support strength for the first critical layer, which has an obvious influence on stope strata behavior:

$$\text{Initial instability}: \ P_{T0I} = \frac{m\gamma C_{0I}}{2L_k} = 2.219 \text{ MPa}$$
$$\text{periodic instability}: \ P_{T1I} = \frac{m\gamma C_{1I}}{2L_k} = 1.008 \text{ MPa}$$

The requirement of the support strength for the second critical layer, which has obvious influence on stope strata behavior:

$$\text{Initial instability}: \ P_{T0II} = \frac{m\gamma C_{0II}}{2L_k} = 2.361 \text{ MPa}$$
$$\text{periodic instability}: \ P_{T1I} = \frac{m\gamma C_{1I}}{2L_k} = 0.768 \text{ MPa}$$

(4)　Determination of support type

ZY21000/38/82D hydraulic support is selected, and its main technical parameters are shown in Table 4.

Table 4. Main Parameters of ZY21000/38/82D Hydraulic Support.

Pattern	Standing Shield Hydraulic Support
Height (lowest/highest)	3800/8200 mm
Total weight of support	78.3 t
Center distance	2050 mm
Working resistance	21,000 kN
Support strength	≥1.65 Mpa
Floor specific pressure	≤5.0 Mpa
Initial support force	16,546 kN
Maneuverability pattern	Electrohydraulic control
Step distance	865 mm
Leg piece	Three telescopic (2 columns)

With the advance of the working face, the change curve of the mining height and the support working resistance is shown in Figure 12. The average mining height of the support resistance monitoring of the 108 working face reached 6.5 m on the 53rd day, 6.9 m on the 57th day, and 7.5 m locally. When the mining height is 5.5~6.5 m, the mining face advancing speed is 8.6 m/d. When the mining height is 6.5~7.5 m, the mining face advancing speed is 9.6 m/d. From day 53 to day 60, the average daily working resistance of the bracket was 11,491 kN (26 MPa), the maximum working resistance was 20,970 kN (47.5 MPa), and the average maximum working resistance was 18,569 kN (42.1 MPa).
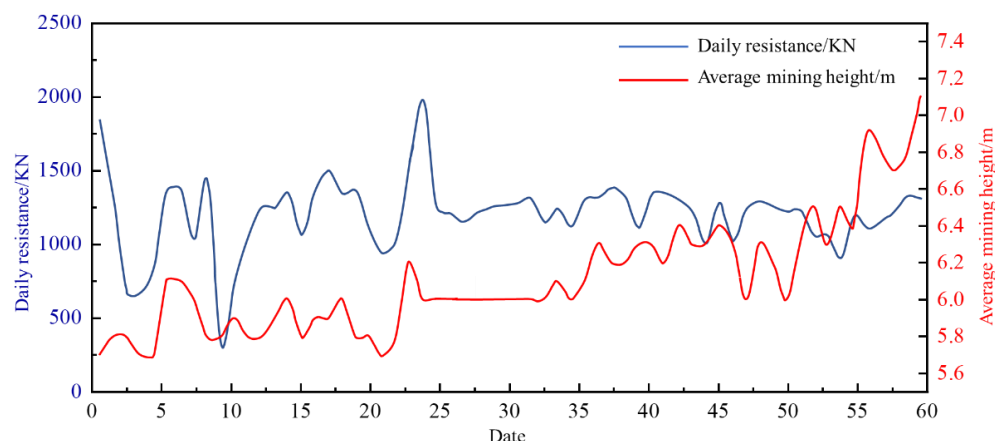
Figure 12. Relationship between mining height and support working resistance.

Due to the instantaneous action of the hydraulic support, the initial support force and the maximum working resistance of the supports are achieved in a short time. However, the working resistance of the support generally conforms to the normal distribution, and the working state of the supports is reasonable. The initial support force meets the needs for the timely roof protection of the supports. The load of the supports is full, and the resistance of the supports is fully exerted.

4.3. Correlation Analysis between Periodic Weighting and Support Load

During the whole mining period, the monitoring system has carried out real-time online monitoring on the mining face circulating working resistance, support load, and its support frequency interval. The resistance data monitoring of the fully mechanized working face is shown in Figure 13.
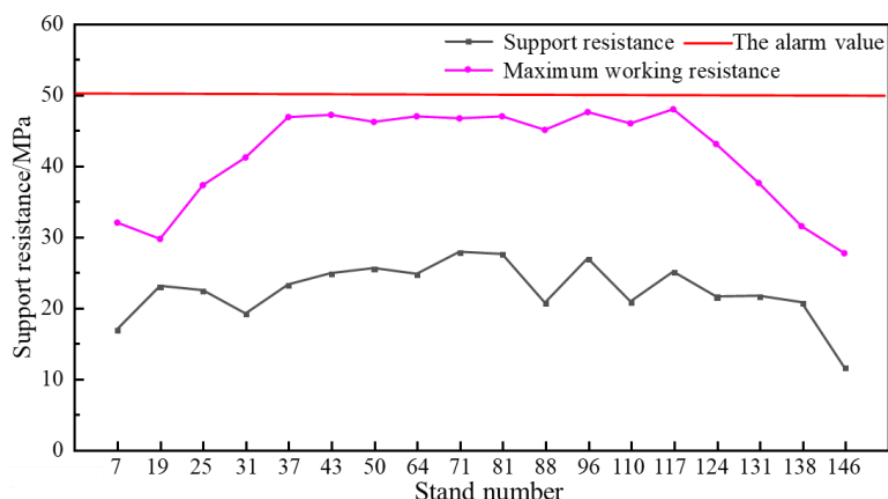
Figure 13. Resistance data monitoring chart of fully mechanized mining.

It can be seen from Figure 13 that the load of the middle support is larger than that of the upper and lower ends of the mining face. The average working resistance of the whole fully mechanized mining is 22.6 MPa, and the maximum occurs in No. 117 support, and the maximum working resistance is 47.9 MPa.

Figure 14 is the frequency distribution of different loads on the fully mechanized mining support. It can be seen from the figure that the working resistance of the supports accounts for a large proportion of 0~5 MPa. It shows that the support moving process is long, and the supports are not moved and lifted in time after mining according to the regulations, and the qualified rate of the initial support force is low. The frequency of 20~30 MPa is the highest, indicating that the normal working resistance of the mining face is between 20 and 30 MPa. The frequency of the supports above 30 MPa is low, indicating that the weighting time of the working face is short, and the weighting duration is not long. However, some supports have low initial support force in some specific time periods. Therefore, the operation process of supports should be strictly managed to give full play to the performance of the supports.

According to the field monitoring data, the average working resistance of Table 5. The 108 working face is 22.00 MPa, the criterion of weighting is 29.86 MPa, and the reasonable support strength should be 37.86 MPa. In this month, the value of the pressure was more than 11 times, the pressure range concentrated in 50~117 supports.

Table 5. Summary of reasonable support strength during periodic weighting.

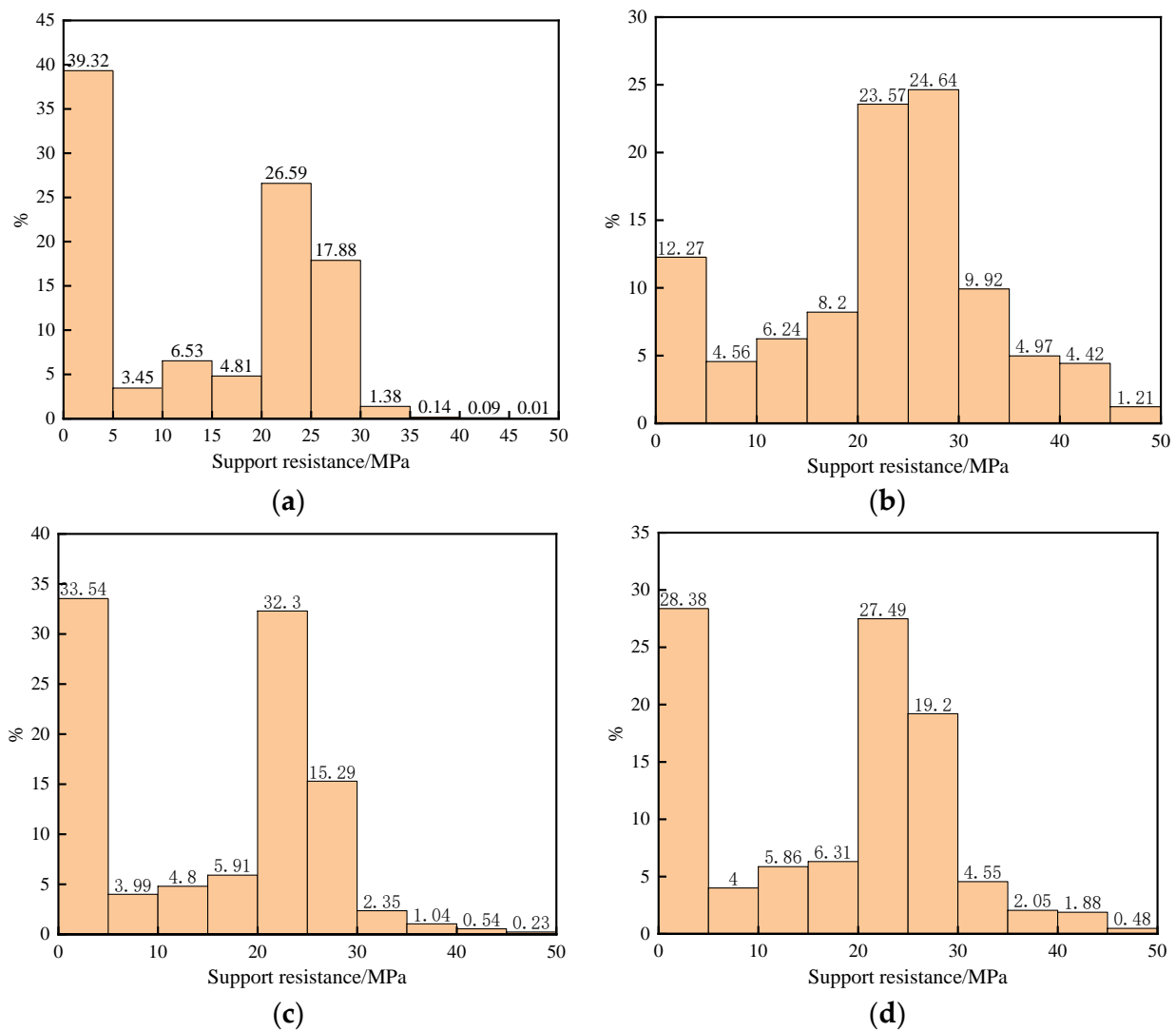| Pressure Station Number	Working Resistance P/MPa	Pressure Criterion $/P + \sigma$	Reasonable Support Strength/$P + 2\sigma$
4	22	31	39
6	23	30	37
9	14	23	33
11	28	35	41
13	21	31	42
16	21	27	33
17	25	32	40
mean value	22.00	29.86	37.86

Figure 14. Statistical histogram of load frequency analysis. (**a**) Pressure monitoring of fully mechanized supports (upper part). (**b**) Pressure monitoring of fully mechanized supports (middle part). (**c**) Pressure monitoring of fully mechanized supports (lower part). (**d**) Integral pressure monitoring of fully mechanized supports.

5. Conclusions

Focusing on the problem of surrounding rock control and support stability in ultra-large height mining face, this study analyzed the calculation of mining resistance of ultra-large mining height support. The stability model of ultra-large mining height support is established, and the stability of ultra-large mining height support is studied. Suggestions are put forward for the application of ultra-large mining height support in the field. The following conclusions are drawn:

1. Due to the large increase in the mining thickness of the ultra-large height mining face, the working resistance of the support and the risk of coal wall spalling increased. The equivalent immediate roof is used to calculate the working resistance of the support, and the coal wall spalling is analyzed. It is required that the ultra-large mining height support should have high setting force, working resistance, and support force.

2. The stability analysis of the supports shows that: When selecting the supports, the stability of the supports can be increased by reducing the support gravity center and widening the support base.

3. The working resistance monitoring results show that: The average working resistance of support is 22.6 MPa, which meets the mining requirement of the mining face. The working resistance of the support's load frequency in 0~5 MPa, accounting for a large proportion. It shows that the process of support moving is long, and the initial support force of the support is small. It is still necessary to strengthen management to give full play to the performance of the supports.

Author Contributions: Conceptualization, X.L.; Data curation, S.W.; Funding acquisition, S.W.; Investigation, S.W.; Methodology, X.L.; Resources, X.L.; Software, Q.Q.; Supervision, Q.Q.; Writing—original draft, S.W. All authors have read and agreed to the published version of the manuscript.

Data Availability Statement: The data are available and explained in this article; readers can access the data supporting the conclusions of this study.

Conflicts of Interest: The authors declare no conflict of interest.

References

1. Liu, H.Y.; Zhang, B.Y.; Li, X.L. Research on roof damage mechanism and control technology of gob-side entry retaining under close distance gob. *Eng. Fail. Anal.* **2022**, *138*, 106331. [CrossRef]
2. Li, X.-L.; Chen, S.-J.; Liu, S.-M.; Li, Z.-H. AE waveform characteristics of rock mass under uniaxial loading based on Hilbert-Huang transform. *J. Cent. South Univ.* **2021**, *28*, 1843–1856. [CrossRef]
3. Yin, X.W. Research status of strata control and large mining height fully-mechanized mining technology in China. *Coal Sci. Technol.* **2019**, *47*, 37–45.
4. Kang, Y.S.; Liu, Q.S.; Gong, G.Q. Application of a combined support system to the weak floor reinforcement in deep underground coal mine. *Int. J. Rock Mech. Min. Sci.* **2014**, *71*, 143–150. [CrossRef]
5. Zhou, X.M.; Wang, S.; Li, X.L. Research on theory and technology of floor heave control in semicoal rock roadway: Taking longhu coal mine in Qitaihe mining area as an Example. *Lithosphere* **2022**, *2022*, 3810988. [CrossRef]
6. Zhao, G.; Zhang, B.; Zhang, L.; Liu, C.; Wang, S. Roof Fracture Characteristics and Strata Behavior Law of Super Large Mining Working Faces. *Geofluids* **2021**, *2021*, 1–12. [CrossRef]
7. Du, T.; Nie, W.; Chen, D.; Xiu, Z.; Yang, B.; Liu, Q.; Guo, L. CFD Modeling of Coal Dust Migration in an 8.8-Meter-High Fully Mechanized Mining Face. *Energy* **2020**, *212*, 118616. [CrossRef]
8. Li, M.; Zhang, J.-X.; Huang, Y.-L.; Gao, R. Measurement and numerical analysis of influence of key stratum breakage on mine pressure in top-coal caving face with super great mining height. *J. Cent. South Univ.* **2017**, *24*, 1881–1888. [CrossRef]
9. Lu, C.; Xu, J.; Zhao, H.; Zhang, H.; Zhang, Y.; Chen, M. Floor Disturbance and Failure Characteristics of Super-Large Mining Height Working Face. *Geofluids* **2022**, *2022*, 1279642. [CrossRef]
10. Ren, Z.; Zuo, M. Research on Technology of Supporting in Super-Large Section Cut in Working Face with Large Mining Height. *Adv. Civ. Eng.* **2021**, *2021*, 3304049. [CrossRef]
11. Liu, C.; Li, H.; Mitri, H. Effect of Strata Conditions on Shield Pressure and Surface Subsidence at a Longwall Top Coal Caving Working Face. *Rock Mech. Rock Eng.* **2019**, *52*, 1523–1537. [CrossRef]
12. Xie, P.S.; Wu, Y.P.; Wang, H.W. Stability analysis of incline masonry structure and support around longwall mining face area in steeply dipping seam. *J. China Coal Soc.* **2012**, *37*, 1275–1280.
13. Wang, D.L.; Zeng, X.T.; Wang, G.F.; Li, R. Stability of a face guard in a large mining height working face. *Int. J. Simul. Model.* **2021**, *20*, 547–558. [CrossRef]
14. Wang, J.C.; Wang, Z.H. Systematic principles of surrounding rock control in longwall mining within thick coal seams. *Int. J. Min. Sci. Technol.* **2019**, *29*, 64–70. [CrossRef]
15. Guo, C.H.; Mao, J. Anti-impact load characteristics of two-stage safety valve for hydraulic support. *Ain Shams Eng. J.* **2022**, *13*, 101738. [CrossRef]
16. Liang, M.; Fang, X.; Li, S.; Wu, G.; Ma, M.; Zhang, Y. A fiber Bragg grating tilt sensor for posture monitoring of hydraulic supports in coal mine working face. *Measurement* **2019**, *138*, 305–313. [CrossRef]
17. Wang, Z.H.; Wang, J.C.; Yang, Y.; Tang, Y.S.; Wang, L. Mechanical relation between support stiffness and longwall face stability with in fully-mechanized mining faces. *J. China Univ. Min. Technol.* **2019**, *48*, 258–267.
18. Yang, K.; Chi, X.L.; Liu, S. Instability mechanism and control of hydraulic support in fully mechanized longwall mining with large dip. *J. China Coal Soc.* **2018**, *43*, 1821–1828.
19. Zeng, X.T.; Meng, G.Y.; Zhou, J.H. Analysis on the pose and dynamic response of hydraulic support under dual impact loads. *Int. J. Simul. Model.* **2018**, *17*, 69–80. [CrossRef]

20. Meng, Z.S.; Zhang, J.M.; Xie, Y.Y.; Lu, Z.G.; Zeng, Q.L. Analysis of the force response of a double-canopy hydraulic support under impact loads. *Int. J. Simul. Model.* **2021**, *20*, 766–777. [CrossRef]

21. Zhang, K.; Li, Y.; Feng, L.; Meng, X.; Zhong, D.; Huang, L. Roof deformation characteristics and experimental verification of advanced coupling support system supporting roadway. *Energy Sci. Eng.* **2022**, *10*, 2397–2419. [CrossRef]

22. Xie, S.R.; Li, S.J.; Wei, Z.; Sun, Y.J.; Zhang, G.C.; Song, B.H.; He, F.L.; Tian, C.Y. Stability control of support-surrounding rock system during fully mechanized caving face crossing abandoned roadway period. *J. China Coal Soc.* **2015**, *40*, 502–508.

23. Cheng, J.-Y.; Zhang, Y.-D.; Cheng, L.; Ji, M.; Gu, W.; Gao, L.-S. Study of loading and running characteristic of hydraulic support in underhand mining face. *Arch. Min. Sci.* **2017**, *62*, 215–224. [CrossRef]

24. Wang, X.; Yang, Z.; Feng, J.; Liu, H. Stress analysis and stability analysis on doubly-telescopic prop of hydraulic support. *Eng. Fail. Anal.* **2013**, *32*, 274–282. [CrossRef]

25. Kong, D.Z.; Cheng, Z.B.; Zheng, S.S. Study on the failure mechanism and stability control measures in a large-cutting-height coal mining face with a deep-buried seam. *Bull. Eng. Geol. Environ.* **2019**, *78*, 6143–6157. [CrossRef]

26. Duan, H.; Zhao, L. Prevention Technology for Strong Mine Pressure Disaster in the Hard-Roof Large-Mining-Height Working Face. *Shock Vib.* **2020**, *2020*, 8846624. [CrossRef]

27. Yang, Z.K.; Sun, Z.; Jiang, S.B.; Mao, Q.H.; Liu, P.; Xu, C.Z. Structural analysis on impact-mechanical properties of ultra-high hydraulic support. *Int. J. Simul. Model.* **2020**, *19*, 17–28. [CrossRef]

28. Yuan, Y. Stability control mechanism of support-surrounding rocks at fully mechanized mining face with great cutting height. *J. China Coal Soc.* **2011**, *36*, 1955–1956.

29. Wu, F.-F.; Liu, C.-Y.; Yang, J.-X. Mode of overlying rock roofing structure in large mining height coal face and analysis of support resistance. *J. Cent. South Univ.* **2016**, *23*, 3262–3272. [CrossRef]

30. Yuan, H.H.; Shan, R.L.; Su, X.G. Deformation characteristics and stability control of a gateroad in fully mechanized mining with large mining height. *Arab. J. Geosci.* **2018**, *11*, 767. [CrossRef]

31. Zhang, Q.; Yue, J.; Liu, C.; Feng, C.; Li, H. Study of automated top-coal caving in extra-thick coal seams using the continuum-discontinuum element method. *Int. J. Rock Mech. Min. Sci.* **2019**, *122*, 104033. [CrossRef]

32. Meng, Z.; Zeng, Q.; Gao, K.; Kong, S.; Liu, P.; Wan, L. Failure analysis of super-large mining height powered support. *Eng. Fail. Anal.* **2018**, *92*, 378–391. [CrossRef]

33. Wu, F.; Yue, X.; Yang, J.; Du, B.; Zhang, J.; Lv, B. Model of overlying strata structure in large mining height excavating condition and calculation of support working resistance. *Geofluids* **2022**, *2022*, 5894735. [CrossRef]

34. Pang, Y.; Wang, G.; Yao, Q. Double-factor control method for calculating hydraulic support working resistance for longwall mining with large mining height. *Arab. J. Geosci.* **2020**, 13. [CrossRef]

35. Li, H.; Kang, T.H.; Li, X.B.; Yang, Y.K.; Wu, L.L. Study on setting load of powered support in high cutting fully-mechanized coal mining face affected to coal wall stability. *Coal Sci. Technol.* **2016**, *44*, 67–71, 92.

36. Wang, G.F.; Li, X.Y.; Zhang, C.C.; Ren, H.W. Research and development and application of set equipment of 8 m large mining height fully—Mechanized face. *Coal Sci. Technol.* **2017**, *45*, 1–8.

37. Wang, G.F.; Pang, Y.H.; Li, M.Z.; Ma, Y.; Liu, X.H. Hydraulic support and coal wall coupling relationship in ultra large height mining face. *J. China Coal Soc.* **2017**, *42*, 518–526.

38. Pang, Y.H.; Wang, G.F. Hydraulic support with large mining height structural optimal design and adaptability analysis. *J. China Coal Soc.* **2017**, *42*, 2518–2527.

39. Gong, P.L.; Jin, Z.M. Study on the structure characteristics and movement laws of overlying strata with large mining height. *J. China Coal Soc.* **2004**, *1*, 7–11.

40. Ralston, J.; Reid, D.; Hargrave, C.; Hainsworth, D. Sensing for advancing mining automation capability: A review of underground au-tomation technology development. *Int. J. Min. Sci. Technol.* **2014**, *24*, 305–310. [CrossRef]

41. Yan, S.H.; Yin, X.W.; Hu, G.J.; Liu, Q.M. Roof structure of short cantilever-articulated rock beam and calculation of support resistance in full-mechanized face with large mining height. *J. China Coal Soc.* **2011**, *36*, 1816–1820.

42. Li, X.L.; Chen, S.J.; Wang, S. Study on in situ stress distribution law of the deep mine taking Linyi Mining area as an example. *Adv. Mater. Sci. Eng.* **2021**, *9*, 5594181. [CrossRef]